Observation of an Interedge Magnetoplasmon Mode in a Degenerate Two-Dimensional Electron Gas

G. Sukhodub,* F. Hohls, and R. J. Haug

Institut für Festkörperphysik, Universität Hannover, Appelstrasse 2, D-30167 Hannover, Germany

(Received 6 July 2004; published 1 November 2004)

We study the propagation of edge magnetoplasmons by time-resolved current measurements in a sample which allows for selective detection of edge states in the quantum Hall regime. At filling factors close to $\nu = 3$ we observe two decoupled modes of edge excitations, one of which is related to the innermost compressible strip and is identified as an interedge magnetoplasmon mode. From the analysis of the propagation velocities of each mode the internal spatial parameters of the edge structure are derived.

DOI: 10.1103/PhysRevLett.93.196801 PACS numbers: 73.43.Lp, 73.20.Mf

Low-frequency collective excitations of the charge density in a two-dimensional electron system (2DES) in a magnetic field travel along the edge of the sample and are called edge magnetoplasmons (EMP's). Since their first observation by Allen *et al.* [1] EMP's have been extensively studied both theoretically [2–4] and experimentally [4–6]. An interedge magnetoplasmon (IEMP) mode [7,8] attributed to the excitations of the boundary between two regions with constant but different charge densities was experimentally observed up to now only in a classical system of surface electrons on helium [9,10].

In a degenerate 2DES under quantum Hall effect conditions different density profiles separated by incompressible strips with constant charge densities appear [11]. The influence of edge channels (EC's) on the propagation of EMP's was addressed in experiments on screened 2DES's in the frequency domain [5,12] and in the time domain [6,13]. The splitting of an incident voltage pulse into several EMP modes propagating with different velocities was observed in unscreened samples [14]. The additional slower modes were interpreted as acoustic EMP modes [15]. In none of these experiments with nonclassical systems were IEMP modes identified.

We report here the observation of both EMP and IEMP modes in a screened 2DES in the quantum Hall regime. In our experiment we clearly demonstrate the decomposition of the two-stage rise of the observed current pulse in the vicinity of the bulk filling factor $\nu = 3$ into different modes of edge magnetoplasmons. Using selective detection of edge states we can distinguish two wave packets of edge excitations moving with different velocities near the sample boundary (Fig. 1). The faster one propagates along the compressible region formed by two strongly coupled outer compressible strips originating from the lowest Landau level. It gives rise to a fundamental EMP mode. The slower wave packet propagates along the inner compressible strip arising from the second Landau level. This wave packet corresponds to an IEMP mode [7,8].

A schematic view of the experimental setup is shown in Fig. 2(a). An AlGaAs/GaAs heterostructure is patterned into a T-shaped form with a width of 200 μm. The 2DES has a carrier concentration $n_s = 1.8 \times 10^{15}$ m^{-2} and a mobility $\mu = 70$ m^2/Vs. A long voltage pulse of 800 ns and typically 2.0 mV amplitude with $\sim$1 ns rise time is applied to the source contact S. With the perpendicular magnetic field pointing into the page it propagates along the upper boundary of the sample to the drain contact D1. A Schottky gate G crosses the entire sample and is situated between S and D1. If a negative voltage is applied to this gate some fraction of the signal is deflected to the other drain contact D2. The distances between source S and each of the drain contacts D1 and D2 are equal and amount to $L = 1.56$ mm. Thus, the transient currents detected at both contacts are directly comparable. In addition, a metallic top gate is deposited on top of the entire sample. The distance d between the top gate and the 2DES is 105 nm. A thin layer of polymethylmethacrylate covering the Schottky gate G isolates the gates from each other in the overlap region. Transmitted pulses are amplified and recorded by a multichannel digital phosphor oscilloscope (DPO). In such a setup the voltage drop at

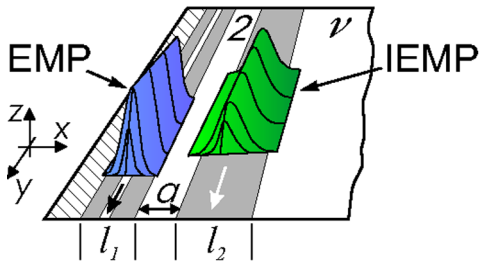

FIG. 1 (color online). Schematic view of EMP and IEMP modes propagating with different velocities and decoupled by an incompressible strip with filling factor $\nu = 2$. Compressible strips are shown as gray areas, incompressible liquids as white areas, and the hatched region represents a depleted semiconductor at the mesa edge.

the input resistance of the preamplifier is proportional to the current through the drain contact.

The scheme of selective detection of EC's is depicted in Fig. 2(b). A bulk filling factor ν is set by the external magnetic field. Here we concentrate on $\nu \approx 3$ since this choice yields the clearest occurrence of the IEMP. The contribution of the entire edge structure can be measured at both drain contacts D1 and D2. In the first case the gate G remains unbiased ($V_G = 0$ mV) and all EC's are transmitted to D1. The local filling factor g under the gate is equal to the bulk value ν [upper sketch in Fig. 2(c)]. In the second case a negative voltage of $V_G = -350$ mV is applied to the gate which depletes the 2DES underneath completely ($g = 0$) deflecting all EC's to D2 [upper sketch in Fig. 2(d)]. To measure the contribution of each Landau level by different contacts the filling factor $g = 2$ is established under the gate G [this situation is depicted in Fig. 2(b)]. In this configuration the two outer EC's formed by the lowest Landau level are transmitted to D1 and the innermost EC is deflected to D2.

Figure 2 represents the main finding of our study, where the decomposition of the two-stage rise of the pulse into two single modes is demonstrated. The time-resolved currents for $\nu = 2.83$ detected at contacts D1 and D2 are shown in panels 2(c) and 2(d), respectively. The origin of the time axis $t = 0$ corresponds to the application of the pulse to the source S. The upper solid curves in both panels represent the signal carried by the entire edge structure. Though different contact pairs were used to detect these traces they closely resemble each other. In both cases the delay time t_0, which is the traveling time of the signal between source and drain, is equal to $t_0 = 4.63 \pm 0.14$ ns, and the first steep rise saturates completely after $t = 30$ ns to $I_1 = (2.02 \pm 0.03)(e^2/h)V_{in}$, where $V_{in} = 2.0$ mV is the pulse amplitude. This first step is followed by a slower rise which develops at $t > 70$ ns and saturates to $I = I_1 + I_2$ with $I_2 = (0.92 \pm 0.04)(e^2/h)V_{in}$ for this filling factor.

The current associated with edge channels originating from the lowest Landau level only is represented by the lower dashed curve in Fig. 2(c). In its initial part it bears a strong similarity to the upper curve: after $t = 30$ ns the current saturates to $2(e^2/h)V_{in}$. For longer times it remains constant as in the case of $\nu = 2$. The second slower rise is completely missing in this trace. The current pulse arrives at D1 as a single wave packet without being redistributed over the whole edge structure. The initial parts of both curves in Fig. 2(c) reveal minor differences (note the logarithmic scale of t in the figure). Namely, the dashed curve ($g = 2$) is delayed by $\sim$1.0 ns and shows a slight change in the slope of the rising part. The first issue is related to the reduced charge density under the gate. This leads to a broadening of the edge channels attributed to the lowest Landau level and as a consequence to a lower propagation velocity under the gate. The change in slope

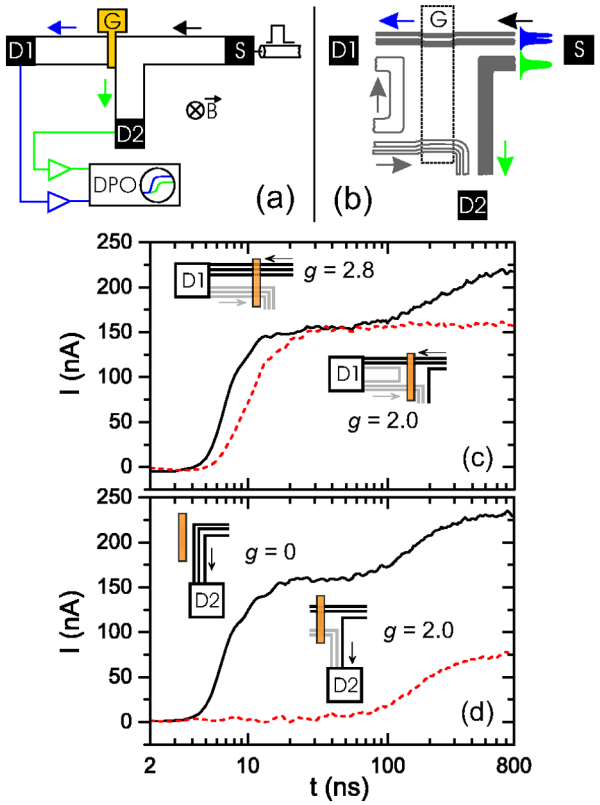

FIG. 2 (color online). (a) Sketch of experimental setup. The metallic top gate which covers the whole area of the sample is omitted for clarity. (b) Scheme of selective detection of edge states. The local filling factor g under the gate G is tuned to $g = 2$. The populated compressible strips are shown as dark areas. (c),(d) Transient currents at $B = 2.70$ T ($\nu = 2.8$) measured at contacts D1 and D2 for the entire edge structure (solid lines in both panels), the two outer EC's (dashed line in (c)), and the inner EC (dashed line in (d)). Sketches along each curve show the configuration of detected edge states.

is probably due to the disturbance of the propagation of edge excitations caused by the negatively biased gate. Nevertheless, the lower curve in Fig. 2(c) reflects the main features of the fast propagating EMP mode.

The lower curve in Fig. 2(d) measured at contact D2 shows the contribution of the inner EC attributed to the upper Landau level. This slower mode has a delay time of $t_0 = 64.0$ ns and saturates to $I_2 \approx (e^2/h)V_{in}$ after several hundred nanoseconds. There is no contribution of the fast mode in this measurement, whereas, it resembles very much the second slower rise in the solid curve in Fig. 2(d). Here we have detected the pure IEMP mode. To our knowledge, this is the first observation of an IEMP mode in time-resolved current measurements in a degenerate 2DES.

The observability of decoupled EMP modes depends on the relation between the widths a, l_1, and l_2 of incompressible and compressible strips (see sketch in Fig. 1) and the distance d from the top gate to 2DES. If the condition $d \ll a, l_1, l_2$ is fulfilled, the electric field associated with

each mode can be assumed to be localized within the corresponding compressible strip and is determined by the gradient of the charge density across this strip [13]. The width of an incompressible strip is substantially smaller than the width of the surrounding compressible ones [11]. It is roughly proportional to the gap ΔE in the energy spectrum of a 2DES in a perpendicular magnetic field. Using the effective g-factor value $|g^*| = 0.44$ for bulk GaAs and $\Delta E = g^* \mu_B B$ we estimate the width $a^{(1)}$ of the incompressible strip with filling factor $\nu^{(1)} = 1$ to be comparable to the magnetic length. Thus, we do not expect to observe decoupled transport due to this strip and, indeed, the contribution of the outer two compressible strips is represented by a single step in our experiment [lower curve in Fig. 2(c)]. The cyclotron gap $\Delta E = \hbar\omega_c$, being significantly larger, gives rise to a broader incompressible strip with $a^{(2)} > 100$ nm facilitating the observation of decoupled edge state transport.

Current traces at different magnetic fields around $\nu = 3$ are shown in Fig. 3 for both modes measured together [Fig. 3(a)] and for each mode measured independently [Fig. 3(b)]. We clearly observe a decrease in the velocity with magnetic field for both modes, although this is much more pronounced for the slower mode. It is remarkable that the fast mode [Fig. 3(b), D1] does not change its form considerably in the filling factor range $3 > \nu > 2$ where its amplitude is ruled by $2e^2/h$. For a quantitative description of the velocities of the fast mode we analyzed the initial parts ($t < 70$ ns) of the current traces corresponding to the entire edge structure [Fig. 3(a)]. The IEMP mode velocities were derived from signals detected at D2 for the case $g = 2$ [lower set of curves in Fig. 3(b)]. The delay time t_0 was obtained from the fit with an exponential decay function [16]. The velocities of EMP and IEMP modes calculated from the delay times by $v = L/t_0$ are presented in Figs. 4(a) and 4(b). At $\nu < 3$ the velocity of the fast mode decreases monotonously achieving a value of 150 km/s at filling factor $\nu = 2$. The velocity of the slower mode decreases proportional to $1/(B - B_0)$ with $B_0 = 2.48$ T. For $B > 2.80$ T it cannot be observed any more in our measurement window of 800 ns.

The velocities of (I)EMP modes can be phenomenologically described by $v \approx (e\Delta n/B)(\alpha/\epsilon_0\epsilon_r)$ where Δn is the difference in the charge density on both sides of the propagation region of each mode and $\alpha \leq 1$ is a parameter which depends on the shape of the density profile [9]. Taking $a^{(2)}$ as the separating strip between the two modes, the ratio $\Delta n^{\mathrm{EMP}}/\Delta n^{\mathrm{IEMP}}$ grows from 2.0 to 2.73 when the magnetic field increases from 2.55 to 2.80 T. This change cannot explain the experimentally observed larger difference in the velocities: $v^{\mathrm{EMP}}/v^{\mathrm{IEMP}}$ varies from 3.3 to 17.5 in this range of magnetic fields. Therefore, different shapes of density profiles α^{EMP} and α^{IEMP} and their significant change with magnetic field have to be taken into account. Such magnetic field dependence is in accordance with the EC picture of the quantum Hall effect, where the compressible regions of varying charge density are expected to get broader with increasing field [11].

To estimate the spatial extension of the density profile for each mode we use a local capacity approximation developed in Ref. [13]. It connects the group velocity v_g of the EMP wave packet with the width l of the propagation region and the distance d between the 2DES and the metallic top gate:

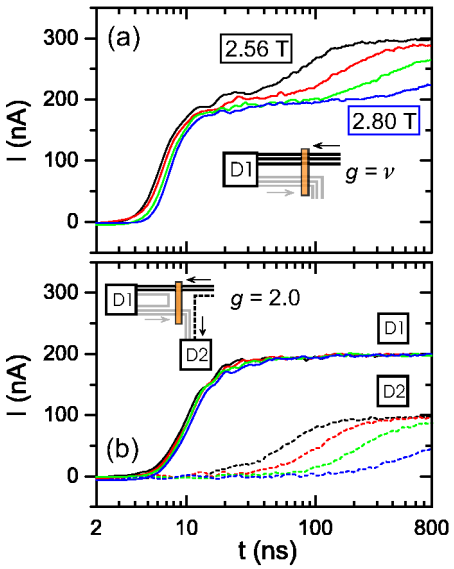

FIG. 3 (color online). Time-dependent currents measured at $B = 2.56$, 2.64, 2.72, and 2.80 T ($\nu = 2.99$, 2.90, 2.81, and 2.73) for the entire edge structure (a) and for the contributions of the outer and inner compressible regions attributed to EMP and IEMP modes (b). The input pulse voltage is $V_{in} = 2.5$ mV.

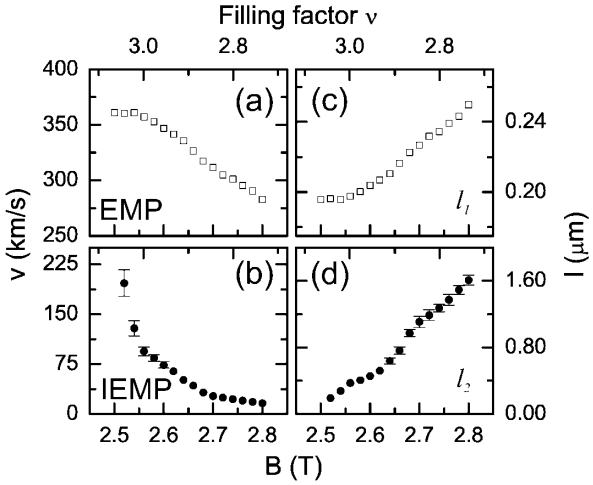

FIG. 4. Velocities of edge magnetoplasmons (a) and interedge magnetoplasmons (b). Right part shows calculated widths of compressible regions arising from the first (c) and the second (d) Landau levels according to Eq. (1).

$$v_g = \frac{\partial \omega}{\partial k} = \frac{e^2 \Delta \nu}{h} \frac{d}{\epsilon_0 \epsilon_r l}, \quad d \ll l, \tag{1}$$

where $\Delta\nu$ is the difference between the filling factors of the restricting isolating regions to the left and to the right of the propagation strip. For the EMP mode $\Delta\nu = g - 0 = 2$; for the IEMP we take $\Delta\nu = \nu - g$. The magnetic field dependence of the (I)EMP velocities manifests itself in the increase of the widths l_1 and l_2 according to Eq. (1). The calculated widths of the propagation regions associated with the EMP and the IEMP modes are shown in Figs. 4(c) and 4(d). The obtained values exceed substantially the distance to the top gate for both modes justifying the local capacity approach. The width of the outer compressible strip can be estimated from theory [11]. We obtain $l_1 = 190$ nm at $B = 2.5$ T increasing to $l_1 = 277$ nm at $B = 2.7$ T. This agrees quite reasonably with the experimental result for the EMP mode [Fig. 4(c)]. The observed plateaulike structure at $\nu > 3$, however, cannot be appropriately accounted for by a theory, where the widths of compressible strips depend monotonously on the magnetic field.

In our experiment we observe a distinct transition from coupled ($\nu > 3.1$; [17]) to decoupled ($\nu < 3.1$) transport regimes, when the IEMP mode shows up. The decoupling of the innermost edge state is known to be asymmetric with respect to the quantum Hall plateau. The authors of Ref. [18] proposed a hybridization of the current-carrying edge states with localized states of the same Landau level when this level approaches the Fermi energy. Then, the wave function of the innermost EC increases its extension and reduces at the same time its amplitude near the edge. This means, on the one hand, a decrease in α^{IEMP} and, on the other hand, an increase in the effective width of the incompressible strip a which enables the observed decoupling. In addition, the spin gap governing $\nu = 3$ can be strongly enhanced by interaction effects influencing the actual charge distribution.

The obtained overall sizes of the edge structure $(l_1 + l_2)$ are of the same order of magnitude as in previous estimates from, e.g., capacitance measurements [19] and scanned potential microscopy [20]. From our analysis, however, we are able to resolve the internal spatial structure of edge states in a range of magnetic fields where their individual contributions can be unambiguously identified.

The decoupled fundamental modes of EMP's assigned to different Landau levels have been recently theoretically treated in Ref. [3]. It was shown that both modes are nearly undamped and propagate with sufficiently different group velocities. The chosen confinement potential, however, was sufficiently steep to neglect the formation of incompressible and compressible strips. Our observed changes in the velocities which are especially strong for the IEMP mode suggest that the spatial extent of the charge density profile connected with each mode must also be taken into account. Here, more theoretical work is necessary.

In summary, we employed selective detection of edge states for time-resolved current measurements under conditions of strongly screened Coulomb interactions. We observed decoupled EMP and IEMP modes propagating along neighboring compressible strips in the vicinity of filling factor 3.

The authors wish to thank R. Winkler for a critical reading of the manuscript and acknowledge financial support by DFG and the BMBF.

*Electronic address for corresponding author: sukhodub@nano.uni-hannover.de

[1] S. J. Allen, Jr., H. L. Störmer, and J. C. M. Hwang, Phys. Rev. B **28**, 4875 (1983).
[2] V. A. Volkov and S. A. Mikhailov, Sov. Phys. JETP **67**, 1639 (1988).
[3] O. G. Balev and P. Vasilopoulos, Phys. Rev. Lett. **81**, 1481 (1998); O. G. Balev, P. Vasilopoulos, and N. Studart, J. Phys. Condens. Matter **11**, 5143 (1999).
[4] *Edge Excitations of Low-Dimensional Charged Systems*, edited by Oleg Kirichek (Nova Science Publishers, Huntington, NY, 2000).
[5] V. I. Talyanskii, A. V. Polisski, D. D. Arnone, M. Pepper, C. G. Smith, D. A. Ritchie, J. E. F. Frost, and G. A. C. Jones, Phys. Rev. B **46**, 12427 (1992).
[6] N. B. Zhitenev, R. J. Haug, K. v. Klitzing, and K. Eberl, Phys. Rev. Lett. **71**, 2292 (1993).
[7] S. A. Mikhailov and V. A. Volkov, J. Phys. Condens. Matter **4**, 6523 (1992).
[8] S. A. Mikhailov, JETP Lett. **61**, 418 (1995).
[9] P. K. H. Sommerfeld, P. P. Steijaert, P. J. M. Peters, and R. W. van der Heijden, Phys. Rev. Lett. **74**, 2559 (1995).
[10] O. I. Kirichek and I. B. Berkutov, Low Temp. Phys. **21**, 305 (1995).
[11] D. B. Chklovskii, B. I. Shklovskii, and L. I. Glazman, Phys. Rev. B **46**, 4026 (1992).
[12] V. I. Talyanskii, D. R. Mace, M Y. Simmons, M. Pepper, A. C. Churchill, J. E. F.Frost, D. A. Ritchie, and G. A. C. Jones, J. Phys. Condens. Matter **7**, L435 (1995).
[13] N. B. Zhitenev, R. J. Haug, K. v. Klitzing, and K. Eberl, Phys. Rev. B **52**, 11277 (1995).
[14] G. Ernst, R. J. Haug, J. Kuhl, K. von Klitzing, and K. Eberl, Phys. Rev. Lett. **77**, 4245 (1996).
[15] I. L. Aleiner and L. I. Glazman, Phys. Rev. Lett. **72**, 2935 (1994).
[16] G. Sukhodub, F. Hohls, and R. J. Haug, Physica (Amsterdam) E **22**, 189 (2004).
[17] G. Sukhodub, F. Hohls, and R. J. Haug (to be published).
[18] B. W. Alphenaar, P. L. McEuen, R. G. Wheeler, and R. N. Sacks, Phys. Rev. Lett. **64**, 677 (1990).
[19] S. Takaoka, K. Oto, H. Kurimoto, K. Murase, K. Gamo, and S. Nishi, Phys. Rev. Lett. **72**, 3080 (1994).
[20] K. L. McCormick, M. T. Woodside, M. Huang, M. Wu, P. L. McEuen, C. Duruoz, and J. S. Harris, Phys. Rev. B **59**, 4654 (1999).